Unique Crystal Structure and Anomalous Magnetic Behavior of Quaternary $U_2ScB_6C_3$

V. H. Tran,*,† P. Rogl,‡ T. Mori,§ H. Ripplinger,|| and K. Schwarz

W. Trzebiatowski Institute of Low Temperature and Structure Research, Polish Academy of Sciences, P.O. Box 1410, 50-950 Wrocław, Poland, Institute of Physical Chemistry, University of Vienna, Währingerstr. 42, A-1090 Wien, Austria, National Institute for Materials Science, Namiki 1-1, Tsukuba, 305-044, Japan, Institute of Physical and Theoretical Chemistry, Vienna University of Technology, Getreidemarkt 9/156, A-1060 Wien

Received May 9, 2008. Revised Manuscript Received June 15, 2008

The crystal structure of the quaternary uranium-based intermetallic $U_2ScB_6C_3$ was derived from X-ray single-crystal counter data. The compound crystallizes in a unique structure type with the space group *P6/mmm*. The unit cell dimensions are as follows: $a = 0.65096(2)$ nm and $c = 0.34265(2)$ nm. Specific heat of the nonmagnetic phonon reference $Th_2ScB_6C_3$ and measurements of the magnetic susceptibility, magnetization, specific heat, and electrical resistivity on polycrystalline sample $U_2ScB_6C_3$ are reported. The experimental data revealed that $Th_2ScB_6C_3$ possesses low-lying optical modes, whereas $U_2ScB_6C_3$ with enhanced electronic specific-heat coefficient at low temperatures ($\gamma = 40$ mJ/mol$_U$·K^2) orders ferromagnetically below $T_C = 61(0.5)$ K, followed by presumably a spin reorientation below 45 K. The investigated $U_2ScB_6C_3$ compound is characterized by an easy-plane anisotropy, which is evidenced by the experimental data and is consistent with the two-ion anisotropic interaction theory. The temperature dependencies of magnetization, specific heat, and electrical resistivity of $U_2ScB_6C_3$ were analyzed with help of the spin-wave theory and compared to the closely related β-UB_2C compound. The magnetism of $U_2ScB_6C_3$ is attributed to the polarized $5f^3$ states and a strong hybridization of the U 6d with B/C 2p states. Band structures using the FLAPW+LO approach were calculated for $Th_2ScB_6C_3$ and $U_2ScB_6C_3$. The theoretical data confirm the metallic properties for all studied compounds and magnetic ground state in $U_2ScB_6C_3$.

Introduction

Compounds with p-electron metalloids (M) and alkali and those with alkaline earth metal (A) form in a rich variety of crystal structures.[1] Most of them belong to a class of so-called Zintl phases, and their electronic structures are rather well-determined based on an electron counting rule. However, when the A element is changed by a transition metal (T) or f electron metal (R, rare earth/An, actinoids), new characteristics of chemical bonding appear, and therefore the electronic structure of the compounds dramatically changes. In the ionic-like Zintl phase compounds, the physical properties are influenced by the covalent bonding of M ions, whereas in the T−M and R−M or An−M compounds, the hybridized metallic d/f-sp bonding plays a key role. As a consequence of the changing bonding characteristics, many new exotic phenomena, including Kondo effect (for instance, in $CeAl_2$[2]), spin fluctuation (UAl_2[3]), heavy-fermion behavior ($CeAl_3$[4]), and superconductivity (UGe_2[5,6]), occur. The appearance of superconductivity in the latter compound, and in two other uranium-based URhGe[7] and UIr,[8] is unexpected owing to the coexistence of ferromagnetism and unconventional superconductivity. A particularly interesting feature is the fact that in all cases the Curie temperature T_C is always higher than the superconducting critical temperature T_{SC}. However, there are only three known compounds with such behavior, so we are still far from understanding the nature of coexisting superconductivity with ferromagnetism. Naturally, any comparative study on itinerant electron ferromagnets is highly desired. In this context we have recently reported on fundamental physical properties of itinerant ferromagnetism in β-UB_2C close to a superconducting transition.[9,10] β-UB_2C is a high-temperature modification adopting the rhombohedral ThB_2C-type structure containing

* Corresponding author. E-mail: v.h.tran@int.pan.wroc.pl. Tel.: (4871)3435021. Fax: (4871) 3441029.
† Polish Academy of Sciences.
‡ University of Vienna.
§ National Institute for Materials Science.
|| Institute of Physical and Theoretical Chemistry, Vienna University of Technology.

(1) *Chemistry, Structure and Bonding of Zintl Phases and Ions*; Kauzlarich, S. M., Ed.; VCH Publishers: New York, 1996.
(2) Buschow, K. H. J.; van Daal, H. J. *Phys. Rev. Lett.* **1969**, *23*, 408.
(3) Trainor, R. J.; Brodsky, M. B.; Culbert, H. V. *Phys. Rev. Lett.* **1975**, *34*, 1019.
(4) Andres, K.; Graebner, J. E.; Ott, H. R. *Phys. Rev. Lett.* **1975**, *35*, 1779.
(5) Saxena, S. S.; Agarwal, P.; Ahilan, K.; Grosche, F. M.; Haselwimmer, R. K. W.; Steiner, M. J.; Pugh, E.; Walker, I. R.; Julian, S. R.; Monthoux, P.; Lonzarich, G. G.; Huxley, A.; Sheikin, I.; Braithwaite, D.; Flouquet, J. *Nature (London)* **2000**, *406*, 587.
(6) Huxley, A.; Sheikin, I.; Ressouche, E.; Kernavanoi, N.; Braithwaite, D.; Calemczuk, R.; Flouquet, J. *Phys. Rev. B* **2001**, *63*, 144519.
(7) Aoki, D.; Huxley, A.; Ressouche, E.; Braithwaite, D.; Flouquet, J.; Brison, J.-P.; Lhotel, E.; Paulsen, C. *Nature (London)* **2001**, *413*, 613.
(8) Akazawa, T.; Hidaka, H.; Fujiwara, T.; Kobayashi, T. C.; Yamamoto, E.; Haga, Y.; Settai, R.; Onuki, Y. *J. Phys.: Condens. Matter* **2004**, *16*, L29.
(9) Tran, V. H.; Rogl, P.; André, G.; Bourée, F. *J. Phys.: Condens. Matter* **2006**, *18*, 703.

10.1021/cm801267a CCC: $40.75
Published on Web 08/15/2008

three puckered metal layers per unit cell sandwiched between planar layers of BC nonmetal layers (space group $R\bar{3}m$).[11]

Some time ago, the authors[12,13] reported on hexagonal quaternary boron carbides, $(Th,U)_2ScB_6C_3$, as an ordered variant of the rhombohedral ThB_2C-type structure. The crystal structure of hexagonal $Th_2ScB_6C_3$, which was derived from room-temperature X-ray powder diffractometry, was solved by combined Rietveld and Patterson methods,[12] and was found to adopt a unique structure type with space group *P6/mmm* (unit cell dimensions: $a = 0.660296(7)$ nm, $c = 0.358421(4)$ nm). $U_2ScB_6C_3$ is isotypic and preliminary investigations showed it to be ferromagnetic below $T_C = 56$ K.[13] However, until now, no detailed structural investigations on single crystals were made and no detailed study on physical properties was hitherto pursued. In view of the interesting physical behavior of β-UB_2C and with respect to its close structural relationship with $U_2ScB_6C_3$, it deemed fruitful to investigate the fundamental properties of $U_2ScB_6C_3$. Therefore, we present in this work details on an X-ray single-crystal study and on low-temperature physical properties obtained from measurements of the magnetization and specific heat of polycrystalline $U_2ScB_6C_3$ samples. As we will show below, the substitution of one U atom by one Sc atom in UB_2C results in a new, truly uranium quaternary compound, $U_2ScB_6C_3$, with a unique crystal structure type. Regarding magnetic properties, we conclude that $U_2ScB_6C_3$ exhibits anomalous behavior, with respect to two successive phase transitions. To better understand the close relationship between crystal structure, bonding, and magnetic properties, we have performed band structure calculations using a full potential linear augmented plane wave plus local orbital method for $Th_2ScB_6C_3$ and $U_2ScB_6C_3$. Analyzing the results of theoretical calculations, we give a consistent interpretation of the experimental data.

Experimental Details

Preparation. Polycrystalline samples of $U_2ScB_6C_3$ and $Th_2ScB_6C_3$ were prepared by argon arc-melting of the elements (99.9 mass %) on a water-cooled copper hearth. Prior to melting, the B,C-powder mixture was compacted in a steel die without the use of lubricants. Annealing was performed in a Knudsen-type graphite crucible for 150 h at 1200 °C in a tungsten sheet metal high-vacuum furnace at 10^{-4} Pa. The boron−carbide compound is slightly sensitive to moisture—thus, all handling was performed under argon or under protective water-free liquids (cutting of specimen under glycerine, etc.). Small single-crystal specimens of $U_2ScB_6C_3$, suitable for single-crystal X-ray diffraction experiments, were isolated after mechanical fragmentation of the middle part of the polycrystalline melted ingots.

X-ray and Electron Diffraction. X-ray examination of polycrystalline materials was performed at room temperature in a Guinier-Huber X-ray camera with an Image Plate recording system (Cu Kα radiation) employing an internal standard of 99.9999% pure Si ($a_{Si} = 0.5431065$ nm). Quantitative Rietveld refinements of X-ray powder data were performed employing the FULLPROF program.[14] X-ray powder diffraction at room temperature indicates that the as-cast and annealed samples are single-phased. For single-crystal X-ray diffraction experiments, the single-crystal specimens of $U_2ScB_6C_3$ were glued (covered by glue) freestanding to the tip of a glass rod and were inspected on a GADDS-D8 instrument, which also served for determination of the unit cell dimensions and quality control of the crystal specimens. Single-crystal X-ray intensity data for $U_2ScB_6C_3$ were collected on a four-circle Nonius Kappa diffractometer equipped with a CCD area detector (graphite monochromated Mo Kα radiation, $\lambda = 0.071073$ nm). Orientation matrix and unit cell parameters for a hexagonal crystal system were derived using the program DENZO.[15] Absorption correction was taken from the program SORTAV,[15] and the structure was refined with aid of the SHELXS-97 program system.[16] Crystal structure data are standardized using the program Structure Program Typix.[17] Transition electron diffraction patterns were taken from a crushed splinter of $Th_2ScB_6C_3$ in am Hitachi H-500 TEM operated at 100 kV.

Physical Property Measurements. Magnetization of powdered specimens of $U_2ScB_6C_3$ was measured using a SQUID magnetometer (Quantum Design) in fields up to $\mu_0 H = 5$ T and in the temperature range 1.7−400 K. Specific heat, $C_p(T)$, measurements on polycrystalline samples of $U_2ScB_6C_3$ and $Th_2ScB_6C_3$ were performed in the temperature range 1.8−100 K, using a thermal relaxation method. The specific heat was measured using a Quantum Design Physical Property Measurement System. The specific heat data of $Th_2ScB_6C_3$ were used to subtract the phonon background heat capacity of $U_2ScB_6C_3$. Electrical resistivity was measured on a bar-shaped sample by applying a standard four-probe ac technique at temperatures down to 2 K.

Electronic Band Structure Calculations. Electronic band structure calculations were performed for $U_2ScB_6C_3$ and $Th_2ScB_6C_3$, employing a full-potential linear augmented plane wave (FLAPW) approach based on the density functional theory using the WIEN2K program package.[18] The FLAPW approach was used to solve the Kohn−Sham equations self-consistently and the generalized gradient approximation of Perdew et al.[19] was used to describe the exchange-correlation energy. The atomic sphere radii of U(Th), Sc, B, and C were kept as 2.5(2.5), 2.0, 1.3, and 1.3 au.

Results and Discussion

Structural Investigations and Crystal Chemistry. Although ternary compounds ThB_2C and UB_2C and the quaternary compounds $(Th,U)_2ScB_6C_3$ melt congruently, the sections ThB_2C - "ScB_2C" and β-UB_2C - "ScB_2C" are not quasibinary due to the instability of the high-temperature

(10) Tran, V. H.; Khan, R. T.; Bauer, E.; Rogl, P. *Physica B* **2008**, *403*, 1375.
(11) Rogl, P.; Fischer, P. *J. Solid State Chem.* **1989**, *78*, 294.
(12) Rogl, P.; Mori, T.; Tanaka, T. Structure and Properties of Quaternary $Th_2ScB_6C_3$. Presented at the 16th IUPAC Conference on Thermodynamics, concurrent with the 10th Symposion on Thermodynamics of Nuclear Materials, Dalhousie University, Halifax, Canada, August 6−11, 2000.
(13) Mori, T.; Tanaka, T.; Rogl, P. Crystal Structure and Properties of Quaternary Actinoid Boron Carbides, $Th_2ScB_6C_3$ and $U_2ScB_6C_3$. Proceedings of the International Conference on Actinoids, Japan, 2002. Published in *J. Nucl. Sci. Technol.* **2002**, Suppl. 3, 122.
(14) Roisnel, T.; Rodriguez-Carvajal, J. *Mater.-Sci.-Forum* **2001**, *378*, 118.
(15) *Nonius Kappa CCD, Program Package COLLECT, DENZO, SCALEPACK, SORTAV*; Nonius: Delft, The Netherlands.
(16) Sheldrick, G. M. *SHELXL-97, Program for Crystal Structure Refinement*; University of Göttingen: Germany, 1997; Windows version by McArdle, Natl. Univ. Ireland, Galway.
(17) Parthé, E.; Gelato, L.; Chabot, B.; Penzo, M.; Cenzual, K.; Gladyshevskii, R. *TYPIX - Standardized Data and Crystal Chemical Characterization of Inorganic Structure Types*; Springer: Verlag, 1994.
(18) Blaha, P.; Schwarz, K.; Madsen, G.; Kvasnicka, D.; Luitz, J. *Program for calculating crystal properties, WIEN2k*; Vienna University of Technology: Vienna, 2001; 3-9501031-1-2.
(19) Perdew, J. P.; Burke, K.; Ernzerhof, M. *Phys. Rev. Lett.* **1996**, *77*, 3865.

compound ScB_2C,[20] which decomposes at temperatures below 1700 °C into ScB_2 and ScB_2C_2.[21] Preliminary investigation of the solubility limit of Sc in β-UB_2C revealed random replacement of about 15% of uranium by scandium atoms.[22] Complete indexation of the single-crystal data set for $U_2ScB_6C_3$ prompted a hexagonal unit cell with a lattice relation close to the structure type of ThB_2C (isotypic β-UB_2C): $a(U_2ScB_6C_3) = a(\beta\text{-}UB_2C)$ and $c(U_2ScB_6C_3) = {}^1/_3c(\beta\text{-}UB_2C)$. Systematic extinctions in powder and single-crystal data prompt the possible space groups in high Laue symmetry: *P6/mmm*, $P\bar{6}2m$, $P\bar{6}m2$, *P6mm*, and *P*622, from which the highest symmetric one was chosen for further structure solution and refinement. Heavy uranium atoms were unambiguously located in the 2c sites of *P6/mmm*, leaving the 1a sites for occupation by scandium atoms. Knowledge of the structural chemistry of actinoid (An) boron carbides with the general formula AnB_2C[23] points toward a structure with alternating metal and nonmetal layers. For our model with the short *c*-axis only one nonmetal layer in $z = 0.5$ is possible, for which the nonmetal layer of β-UB_2C (ThB_2C type[11]) seems to be most appropriate for $U_2ScB_6C_3$. The electron density peaks revealed in the difference Fourier synthesis $F_{obs} - F_{U,Sc}$ are fully consistent with this structure model, which refined satisfactorily and finally converged at $R_F^2 = 0.033$. No significant deviation from full atom occupancy was evident.

Refinement, however, prompted a small random replacement of 0.948(4) Sc + 0.052 U1 atoms in the Sc site (1a), indicating a small homogeneity region (~1 at. %) of the quaternary compound, $U_{2+x}Sc_{1-x}B_6C_3$. Moreover, from the calculated anisotropic atomic displacement parameters for the U atoms, we see that vibrating amplitude in the ab plane is larger than that along the *c* axis because $U_{11}(=0.0044 \times 10^{-2}$ nm$^2)$ are larger than $U_{33}(=0.0031 \times 10^{-2}$ nm$^2)$. Concerning displacement parameters for B and C, one expects that these atoms with a large U_{iso} of 0.0052×10^{-2} nm^2 should be vibrating more violently than U and Sc atoms do. Table 1 summarizes the X-ray single crystal data for $U_2ScB_6C_3$.

Rietveld refinement of the X-ray room temperature intensity pattern of $Th_2ScB_6C_3$, reaching low residual values $R_F = 0.032$, $R_I = 0.058$ for a set of 45 independent reflections ($x_B = 0.2637(1)$), proved isotypism with the crystal structure of $U_2ScB_6C_3$. TEM data for $Th_2ScB_6C_3$ confirm the setting of the unit cell. The electron diffraction patterns of the a^*-b^* and a^*-c^* planes in Figure 1 reveal no indication of the existence of superstructures. The Rietveld data for $Th_2ScB_6C_3$ and $U_2ScB_6C_3$ are available on request.

The structure type of $U_2ScB_6C_3$ (see Figure 2) is one of the layer-type boron carbides YB_2C, ThB_2C, and β-UB_2C type:[23] planar 3^6-Kagomé metal layers (U_2Sc) sandwiched between planar nonmetal Kagomé networks $6B(6B + 3C)^2$ in $z = {}^1/_2$. Each boron atom in the structure attains a tetrakaideka-hedral overall co-ordination $[U_4Sc_2B_2C]B$. Co-ordination around the scandium atoms (boron-hexagons, $d_{B-Sc} = 0.2465$ nm close to the sum of radii) resembles AlB_2-type borides (ScB_2). Boron hexagons "sandwiching" the scandium atoms show with $d_{B-B} = 0.1772$ nm practically the sum of the covalent boron radii, 0.1760 nm, whereas the larger uranium atoms are surrounded by a trigonal net unit 6B + 3C consisting of straight boron−carbon−boron bonds ($d_{C-2B} = 0.1483$ nm, $\phi_{BCB} = 180°$) and close B−B bonds ($d_{B-B} = 0.1772$ nm). Carbon atoms are in quadratic bipyramidal co-ordination $[U_4B_2]C$; each carbon atom is closely bonded ($d_{B-C} = 0.1483$ nm) to two neighboring boron atoms. The reduced bond length of $d_{B-C} = 0.1483$ nm suggests a double bondlike behavior. Whereas boron−uranium bonds seem to be weak ($d_{U-B} = 0.2944$ nm), exceeding the sum of radii by about 12%, carbon−uranium distances $d_{U-C} = 0.2543$ nm are slightly shorter than the corresponding sum of radii. The planar network of nonmetal $6B(6B + 3C)^2$ Kagomé atom units in $z = {}^1/_2$ is the same as that encountered in ThB_2C.[11] A proper structural chemical formula is $U_2{}^{[5U+3Sc,12B+6C]}Sc^{[2Sc+6U,12B]}B_6{}^{[2B+C,4U+2Sc]}C_3{}^{[2B,4U]}$. Shortest uranium−uranium distances are along the *c*-axis, $d_{U-U} = 0.34265$ nm and are close to the so-called *Hill* limit.[24] It is interesting to analyze the differences between the structure of $U_2ScB_6C_3$ and β-UB_2C (ThB_2C type). The

Table 1. Single-Crystal Data for $U_{2+x}Sc_{1-x}B_6C_3$; Space Group *P6/mmm*; No. 191; Origin at Center; Anisotropic Atomic Displacement Parameters U_{ij} in [10^2 nm^2]; $B_{ij} = 8\pi^2U_{ij}$

formula from refinement	$U_{2.05}Sc_{0.95}B_6C_3$
data collection; radiation	Nonius Kappa CCD; Mo Kα redundancy > 7
crystal size	28 × 28 × 42 μm^3
density (Mg/m^3)	7.48
a [nm]; *c* [nm]	0.65096(2); 0.34265(3)
data collection, 2Θ range	2 < 2Θ < 72.19°; 90 s/frame
total number of frames	389 for 8 sets; scan width = 2°
reflections in refinement	153 $F_o > 4\sigma(F_o)$ of 153
mosaicity	<0.43
number of variables	10
$R_F^2 = \Sigma\lvert F_0^2 - F_c^2\rvert/\Sigma F_0^2$	0.0334
R_I	0.066
GOF	1.273
extinction (Zachariasen)	0.047(6)
M1 in 1a (0,0,0); occ.	0.948(4) Sc + 0.052 U1
$U_{11} = U_{22}$; U_{33}; U_{12}	0.0044(9); 0.0031(14); 0.0022(4)
U2 in 2c ($^1/_3$,$^2/_3$,0); occ.	1.00 U2
$U_{11} = U_{22}$; U_{33}; U_{12}	0.0043(3); 0.0018(4); 0.0021(1)
B in 6k (x,0,$^1/_2$)	$x = 0.272(1)$
occ.	1.0
U_{iso}	0.0052(11)
C in 3g ($^1/_2$,0,$^1/_2$); occ.	1.0
U_{iso}	0.0050(14)
residual electron density; max; min in [e/nm^3] × 1000	4.4; −8.5

(20) Bauer, J. *J. Less Common Met.* **1982**, *87*, 45.
(21) Shi, Y.; Leithe-Jasper, A.; Tanaka, T. *J. Solid State Chem.* **1999**, *148*, 250.
(22) Rogl, P.; Rupp, B.; Felner, I.; Fischer, P. *J. Solid State Chem.* **1993**, *104*, 337.
(23) Rogl, P. *Ternary Metal Boron Carbon Systems*; Effenberg, G., Ed.; ASM International: Materials Park, OH, 1998; pp 1−525.
(24) Hill, H. H. In *Plutonium 1970 and Other Actinides*; Miner, W. N., Ed.; Nuclear Metallurgy; AIME: New York, 1979; Vol. 17, Part I, p2.

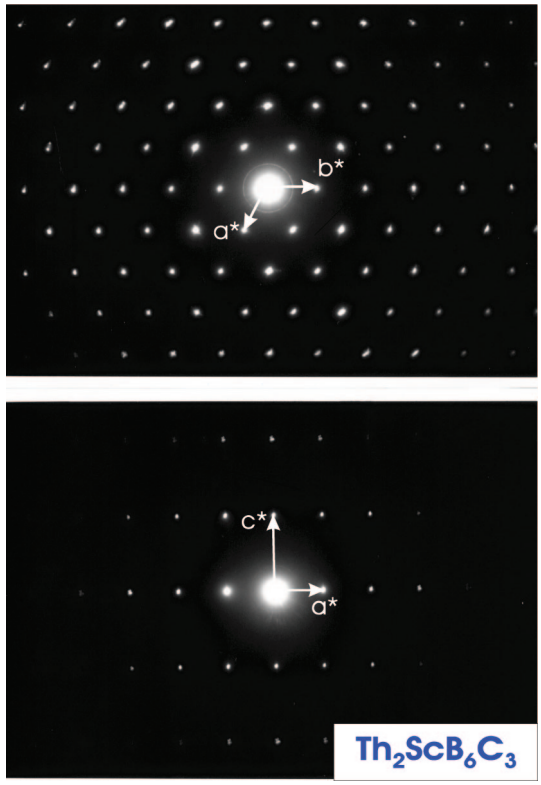

Figure 1. Reciprocal lattice of $Th_2ScB_6C_3$ from transition electron microscopy for plane a^*-b^* (above) and for plane a^*-c^* (below). Note: there are no indications for superstructure spots.

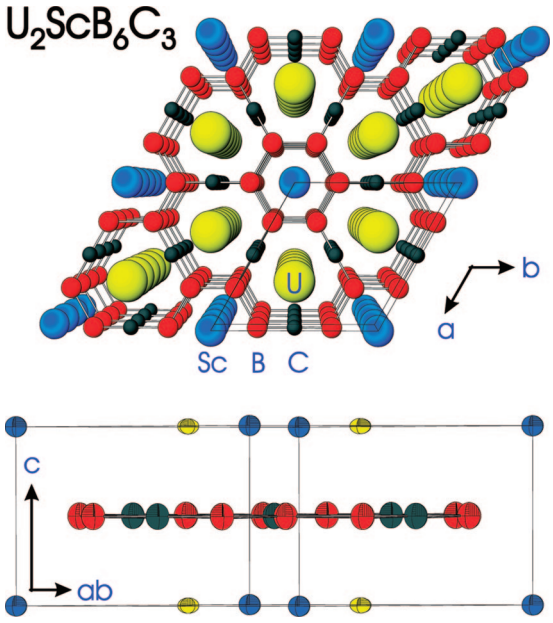

Figure 2. Crystal structure of $U_2ScB_6C_3$ as seen along the c-axis (upper part; atoms are spheres in relation to their radii) and in view perpendicular to the c-axis (lower part; atoms are displayed with their thermal ellipsoids). Note that nonmetal layers and metal layers are planar.

nonmetal layers $6B(6B + 3C)^2$, composed of small B_6 hexagons and large B_6C_3 units are particularly well-adapted to host in between metal atoms of rather unequal size such as Sc ($r_{Sc} = 0.165$ nm) and U ($r_U = 0.175$nm). While the metal layer in $U_2ScB_6C_3$ is perfectly planar, a slightly puckered U layer in β-UB_2C may balance the

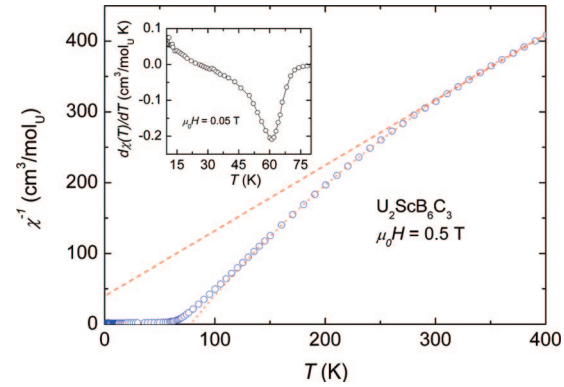

Figure 3. Temperature dependence of the inverse magnetic susceptibility of $U_2ScB_6C_3$ at 0.5 T. The dashed and dotted lines are fits to the Curie−Weiss and modified Curie−Weiss laws, respectively. The inset shows the temperature derivative of the susceptibility at 0.05 T as a function of temperature.

U−B distances to the alternating smaller B_6 and larger B_6C_3 units around the U atom.

Finally, from X-ray single-crystal and X-ray powder diffraction data it is important to stress that $U_2ScB_6C_3$, like $Th_2ScB_6C_3$,[12] are ordered and truly quaternary compounds. Therefore, based on knowledge of the crystallographic data of $U_2ScB_6C_3$, it is highly desired to look for new members of the family involving other actinoid and rare-earth elements.

Physical Properties. Inverse magnetic susceptibility $\chi(T)$ of $U_2ScB_6C_3$ at 0.5 T is shown in Figure 3. It can be seen that the $\chi(T)$ dependence shows a linear behavior above 300 K, implying a localized-like character of the 5f electrons in the compound. From the fitting of the experimental data to the Curie−Weiss (CW) law, $\chi_{CW}(T) = N_A\mu_{eff}^2/[3k_B(T - \Theta_p)]$, where N_A is Avogadro's number and k_B is Boltzmann's constant, we obtained the effective magnetic moment $\mu_{eff} = 2.94(2)\ \mu_B$/U and paramagnetic Curie temperature $\Theta_p = -43(5)$ K. Notice that the observed value of μ_{eff} is essentially small if compared to those of free U^{3+} or U^{4+} ions (3.62 μ_B or 3.58 μ_B); thus, μ_{eff} fits into the picture of itinerant 5f moments. Below room temperature we observe a curvature of the $\chi(T)^{-1}$ dependence. Fitting of the data by a modified Curie−Weiss (MCW) law: $\chi(T) = \chi_{CW}(T) + \chi_0$ could be successful for a much broader temperature range. Here, χ_0 is a temperature-independent susceptibility, including core electron diamagnetism, Pauli paramagnetism, and the Van Vleck terms. The fit of the data between 150 and 400 K yielded $\chi_0 = 8.3 \times 10^{-4}$ mol/cm^3, $\mu_{eff} = 2.04(2)\ \mu_B$, and $\Theta_p = 78(5)$ K. In comparison with β-UB_2C having $\mu_{eff} = 1.45\ \mu_B$ the 5f electrons in $U_2ScB_6C_3$ seem to have a higher degree of localization. However, we must admit that due to magnetocrystalline anisotropy and texture effect a description of the susceptibility of polycrystalline sample in terms of the MCW law should be considered as a parametrization of the data only.

In the inset of Figure 3 we show the temperature derivative of the susceptibility collected at a low field of 0.05 T. The $d\chi(T)/dT$ curve reveals a minimum at $T_C = 61.1$ K, suggesting the existence of a magnetic phase transition of ferromagnetic origin. Apparently, the observed T_C value is slightly higher than that previously reported of 56 K.[13] The

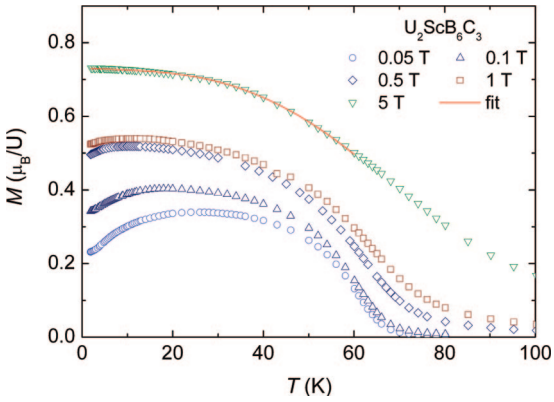

Figure 4. Temperature dependence of the magnetization of $U_2ScB_6C_3$ measured at various magnetic fields. The solid line is a fit to eq 4.

discrepancy probably arises from different methods for the determination of T_C.

The magnetization $M(T)$ at several magnetic fields as a function of temperature is shown in Figure 4. In magnetic fields below 1 T a broad maximum is observed in the magnetization curves. This behavior is typically seen in ferromagnetic systems in which anisotropy and magnetostriction are considerable. When a higher field is applied, the magnitude of the magnetization increases and the position of the inflection point of the magnetization curve shifts to higher temperatures. At a field of 5 T, the minimum of $d\chi(T)/dT$ attains a value of 72 K.

For an itinerant ferromagnet the spin-wave excitation is expected and the magnetization follows the prediction of the Heisenberg model:

$$\frac{M(0)-M(T)}{M(0)} = BT^{3/2} + CT^{5/2} + \ldots \quad (1)$$

The coefficient B and C are related to the spin-wave stiffness constant D:

$$B = 2.612\frac{g\mu_B}{M(0)}\left(\frac{k_B}{4\pi D}\right)^{3/2} \quad (2)$$

$$C = 1.341\frac{g\mu_B}{M(0)}\left(\frac{k_B}{4\pi D}\right)^{5/2}\frac{3\pi\langle r^2\rangle}{4} \quad (3)$$

where g is the Landé factor and $\langle r^2\rangle$ is the average mean square range of the exchange interaction. At low temperatures the spin waves are strongly affected by the presence of anisotropy. Due to the hexagonal crystal structure of the studied compound, there exists a magnetocrystalline anisotropy, which may lead to the appearance of anisotropy gap Δ in the spin-wave spectrum, and the magnetization given by eq 1 is modified as

$$\frac{M(0)-M(T)}{M(0)} = BT^{3/2} + B_1T^{3/2}\exp(-\Delta/k_BT) \quad (4)$$

A fit of the experimental data for the temperature range 2−30 K to eq 4 gave $B = 0.18 \times 10^{-3}$ K$^{-3/2}$ and $\Delta/k_B = 85(5)$ K. Taking $g = 0.67$ for U^{3+}, $V = 135.33$ Å^3, and a saturation moment of 1.02 μ_B (see below), we have estimated the value of the spin-wave stiffness coefficient D to be 51 meV·Å^2. If we apply the same procedure of fitting to the data of β-UB_2C,[9] we get $B = 0.23 \times 10^{-3}$ K$^{-3/2}$ and $\Delta/k_B = 108(5)$ K and coefficient $D = 81$ meV·Å^2 for the latter compound.

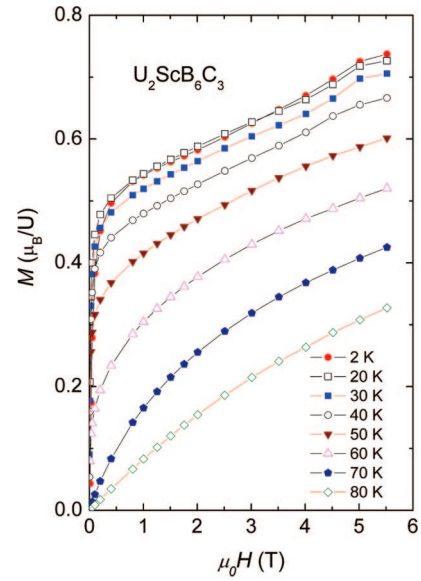

Figure 5. Magnetization of $U_2ScB_6C_3$ measured at several selected temperatures below 80 K.

Thus, the spin-wave stiffness coefficient D of $U_2ScB_6C_3$ is found to be smaller than that for β-UB_2C.

The ratio D/k_BT_C is a measure of the exchange interaction range associated with a shape of the band structure.[25] We calculated this ratio for $U_2ScB_6C_3$ and β-UB_2C to amount to 9.7 and 15 Å, respectively. Smaller values of T_C, D, and D/k_BT_C of $U_2ScB_6C_3$ compared to those of β-UB_2C imply that the magnetic state changes from strong to weak magnetism when one U atom in β-UB_2C is replaced by Sc.

In the case of 3d electron metals, the value of D is given as[26]

$$D = \frac{1}{3n}\left\{\frac{1}{2}[M(\varepsilon_\uparrow) + M(\varepsilon_\downarrow)] - \frac{1}{\Delta}\int_{\varepsilon_\downarrow}^{\varepsilon_\uparrow} M(\varepsilon)\,d\varepsilon\right\} \quad (5)$$

where

$$M(\varepsilon) \propto \sum_\lambda \int_{\lambda k=\varepsilon} \left|\nabla_{\varepsilon\lambda}\right| dS$$

is a surface integral involving the gradient of the single-particle energy, $n = n\uparrow - n\downarrow$ is the excess number of electrons, and Δ is the exchange splitting. The integral of $\nabla_{\varepsilon\lambda}$ is the inverse of the density of states $N(E)$. Comparing the observed value of stiffness for $U_2ScB_6C_3$ with that of β-UB_2C, one suspects that the decrease in D for the studied compound is due to an increase of DOS and/or to a decrease in magnetic splitting Δ.

In Figure 5 we show the magnetization measured at several temperatures up to 80 K. Apparently, the isotherms do not show any saturation at the maximal magnetic fields applied. Magnetization at 2 K and 5.5 T reaches a value of 0.73 μ_B. Comparison of the observed value to that for the U^{3+} ions of $gJ = 2.33$ μ_B implies an itinerant nature of the 5f electrons in $U_2ScB_6C_3$.

To estimate the saturation moment, we have fitted the data to the relation $M(H) = M_s + a/H + b/H^2$, where a and b are constants. For the data above 4.0 T, the fit yielded $M_s =$

(25) Katsuki, A.; Wohlfarth, E. P. *Proc. R. Soc.* **1966**, *295*, 182.
(26) Wakoh, S. *J. Phys. Soc. Jpn.* **1971**, *30*, 1068.

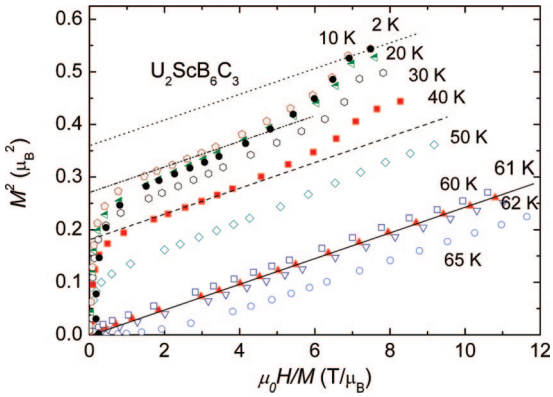

Figure 6. Arrott plot for $U_2ScB_6C_3$. The solid, dashed, dotted-dashed, and dotted lines are guides for the eye.

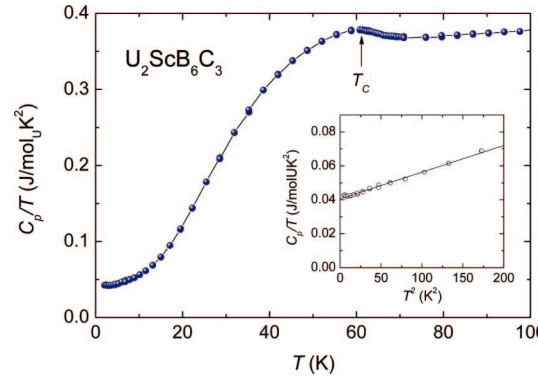

Figure 7. Temperature dependence of the specific heat divided by temperature, $U_2ScB_6C_3$. The inset shows C_p/T vs T^2 at low temperatures.

1.02(5) μ_B, $a = -1.96$ μ_BT and $b = 2.30$ μ_BT^2. It is worthwhile to point out that M at temperatures below 50 K exhibits a change in its slope around 3.5 T. This feature suggests a reorientation of magnetic moments in uranium sublattices. The magnetization curve at 70 K and even at 80 K corresponds to that of material with a strong ferromagnetic correlation, e.g., due to short-range magnetic interactions.

To ascertain exactly the value of Curie temperature, we apply the scheme proposed by Arrott.[27] According to the mean-field theory, the M^2 versus H/M dependence at various temperatures should show a series of parallel lines in accordance with the magnetic equation of state of the form $M^2 = A + B^*H/M$. For ferromagnets, the coefficient $A = 0$ at the Curie temperature. As can be seen in Figure 6, the isotherm at 61 K follows a straight line through the origin of the plot (see solid line). The result confirms the ferromagnetic phase transition in $U_2ScB_6C_3$ at $T_C = 61 \pm 0.5$ K.

It is interesting to note that the $M^2(H/M)$ vs H/M plot deviates from the linearity at temperatures below 50 K. The deviation is illustrated by a dashed line on the 40 K data. At 2 K, the magnetization jump amounts to ~0.06 μ_B compared to the total spontaneous magnetization of ~0.585 μ_B (see the dotted and dotted-dashed lines on the 2 K data). Because the uranium atoms occupy two positions, 2c and 1a, and at the latter position a part of the U atoms of about 5% shares the Sc atoms, we may suspect the magnetization jump is due to contribution of the U magnetic moments at the 1a sites, denoted as U1. Bear in mind the fact that the shortest distance between atoms at 1a sites is 0.3427 nm. This value corresponds to the effective d_{U1-U1} distance of 7.05 nm, being too large to allow the magnetic moments of U1 to form their own magnetic sublattice. Therefore, the appearance of the eventual magnetic moment of U1 would be a result of the induction by U2. However, if the uranium ions at 1a sites carry the same magnetic moment as those in 2c, then the total moment of all U1 ions contributes 0.015 μ_B only, i.e., 4 times smaller than the magnetization jump. Therefore, to explain the jump in the magnetization curves below 50 K, one needs to assume an orientation of magnetic moments of all uranium ions in the unit cell. It is worthwhile to mention a two-transition phenomenon observed in UGe_2[3] and β-UB_2C,[9] both exhibiting a ferromagnetic transition at T_C and a broad maximum at T^* in the magnetic specific heat and temperature derivative of electrical resistivity. In the first compound, it was reported that T^* decreases with pressure and disappears at a pressure at which the superconductivity is strongest.

In Figure 7 we show the temperature dependence of the specific heat of $U_2ScB_6C_3$ at low temperatures in the form C_p/T versus T. We observed a maximum at 61 K, which corroborates the magnetic phase transition found in magnetic measurement. Note that the magnetic transition presents a long tail up to 66 K, suggestive of short-range correlations between the magnetic moments before the long-range ordering sets in. The magnitude of the specific heat jump $\Delta C_p/(\gamma T_C)$ at T_C is small, 0.30(0.02), and supports the above suggestion.

Analyzing the low-temperature data presented in the inset of Figure 7, one recognizes that the specific heat follows the relation

$$C_p = \gamma_{LT}T + \beta T^3 \qquad (6)$$

The least-squares fit of eq 6 to the data between 2 and 10 K yielded $\gamma_{LH} = 40(1)$ mJ/mol$_U$·K^2 and $\beta = 0.1516$ mJ/mol$_U$·K^4. The latter value corresponds to the Debye temperature of $\Theta_D = 413$ K. Using the formula $\gamma = (1/3)\pi^2 k_B^2 N(E_F)$, where $N(E_F)$ is the electronic density of states at the Fermi level, we estimated $N(E_F) = 17.4$ states/eV·at., distinctly larger than the value of 14.7 states/eV·at. in β-UB_2C.[9]

To evaluate the magnetic contribution to the total specific heat, the lattice specific heat has to be subtracted. Because the lattice structures of $U_2ScB_6C_3$ and $Th_2ScB_6C_3$ are isomorphous to each other, we may consider the lattice specific heat of $Th_2ScB_6C_3$ as phonon contribution to the specific heat of $U_2ScB_6C_3$ after scaling by a temperature factor of 0.99 due to their difference in the mole mass. We analyze the specific heat of $Th_2ScB_6C_3$ in the form C_p/T^3 vs T in Figure 8. As can be seen, there are two clear features: The pronounced maximum locates around 30 K in the $C_p/T^3(T)$ curves, indicating some optical mode, and the upturn in C_p/T^3 below 10 K, which conveys a substantial contribution of the electronic specific heat. The best fit results shown as a solid line in Figure 8 were obtained assuming the presence of electronic contribution, acoustical and optical modes. The electronic specific heat coefficient $\gamma = 4.45$ mJ/mol$_{Th}$·K^2 was estimated from the

(27) Arrott, A. *Phys. Rev.* **1957**, *108*, 1394.

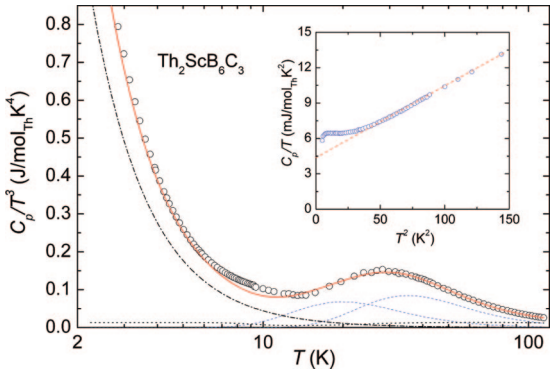

Figure 8. The ratio C_p/T^3 of $Th_2ScB_6C_3$ as a function of temperature. The dashed, dotted, and dash-dotted represent the Einstein, Debye, and electronic contributions, respectively. The solid line is the theoretical curve. The inset shows C_p/T vs T^2. The dashed line is the fit to eq 6.

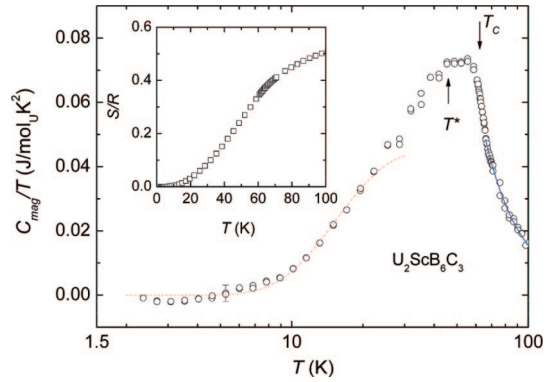

Figure 9. Temperature dependence of the magnetic specific heat of $U_2ScB_6C_3$ divided by temperature. The dashed line is a fit to the spin-wave theory. The inset shows the magnetic entropy vs temperature.

linear fit of the data (see inset of Figure 8). The acoustical modes are represented as Debye oscillators, which contribute to the total specific heat as

$$C_{\mathrm{ph,D}} = 9Rn_{\mathrm{D}}(T/\Theta_{\mathrm{D}})^3 \int_0^{\Theta_{\mathrm{D}}/T} \frac{x^4 \exp(x)}{(\exp(x)-1)^2}\,\mathrm{d}x$$

where R is the gas constant, Θ_D is the Debye temperature, and n_D is number of Debye oscillators. The optical modes are given as

$$C_{\mathrm{ph,E}} = 3Rn_{\mathrm{E}} \frac{(\Theta_{\mathrm{E}}/T)^2 \exp(\Theta_{\mathrm{E}}/T)}{(\exp(\Theta_{\mathrm{E}}/T)-1)^2}$$

where Θ_E and n_E are respectively the Einstein temperature and number of Einstein oscillators. For a compound having n atoms per unit cell, there will be 3 acoustical and $3n - 3$ optical modes. However, for $Th_2ScB_6C_3$ a good description is possible by use of only three modes with $\Theta_D = 895(5)$ K, $n_D = 10$, $\Theta_{E1} = 173(3)$ K, $n_{E1} = 1.6$, and $\Theta_{E2} = 99(2)$ K, $n_{E2} = 0.4$. The results of the fit are shown in Figure 8.

In Figure 9 we show the magnetic contribution, $C_{mag}(T) = C_p(T) - \gamma_{LH}T - C_{ph}(T)$ to the specific heat of $U_2ScB_6C_3$. As can be seen, C_{mag}/T exhibits a plateau between $T^* = 45$ and $T_C = 61$ K. The observation supports two anomalies observed in the magnetization measurements. At low temperatures the magnetic specific heat can be analyzed in terms

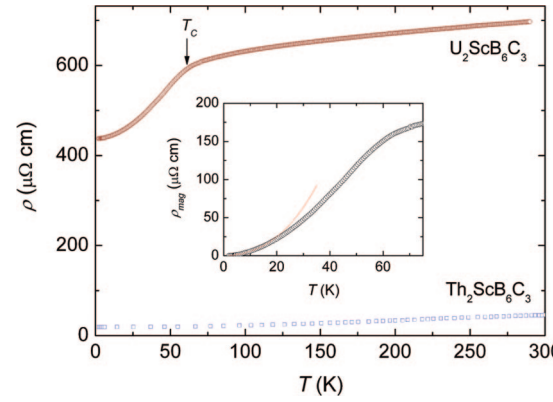

Figure 10. Temperature dependence of the electrical resistivity of $U_2ScB_6C_3$ and $Th_2ScB_6C_3$. The inset shows low-temperature data of the magnetic resistivity of $U_2ScB_6C_3$. The solid line is a fit.

of the spin-wave theory.[28] Accordingly, the spin-wave contribution to the magnetic specific heat $C_{mag}(T)$ of ferromagnets with anisotropic molecular fields will be dominated by an exponential term

$$C_{\mathrm{mag}}(T) = Af(T)\exp(-\Delta/k_{\mathrm{B}}T) \qquad (7)$$

where A is a constant and $f(T)$ is a function, which represents the character and dimensionality of the spin-wave excitation. The function $f(T)$ takes the form of $T^{1/2}$ in an easy axis of anisotropy, but $T^{-1/2}$ in an easy plane. We have fitted the experimental data to eq 7 with both functions $f(T) = T^{1/2}$ and $f(T) = T^{-1/2}$. Based on the reduced χ^2 values of the fits, it is difficult to deduce which type of anisotropy is proper for $U_2ScB_6C_3$. Nevertheless, the gap in the magnon spectrum Δ/k_B was found to be 68 K for the plane anisotropic and 38 K for the easy-axis one; thus, the first value is closer to that deduced from the magnetization data of 85 K. At this point one may recall that the shortest distance between the uranium atoms is along the c-axis. According to the theory developed by Cooper and co-worker[29] for the case of two-ion anisotropic interaction, the hybridization of a pair of magnetic ions with the band electrons gives a piling up of charge along the interionic axis and this determines a preference for alignments of magnetic moments perpendicular to this axis. If the theory of Cooper and co-worker[29] is applicable to $U_2ScB_6C_3$, then the type of anisotropy is easy-plane, and then may support the specific heat data. The magnetic entropy at T_C is small (inset of Figure 9), suggestive also of an itinerant f electron magnetism. Inspecting Figure 9, we see that a noticeable magnetic contribution persists up to at least 100 K. One of the possibilities is the existence of a short-range magnetic correlation far above T_C, for which the observed high-temperature specific heat tail is well-described by a T^{-2} function (drawn as solid line).

The temperature dependence of the electrical resistivity of $U_2ScB_6C_3$ (Figure 10) demonstrates this compound to be metallic. From the resistivity data, one discerns the magnetic phase transition, where the $\rho(T)$ curve exhibits a distinct knee

(28) Akhieza, A. I.; Baýakhtar, V. G.; Peletminskii, S. V. In *Thermodynamics of ferromagnets and antiferromagnets. Spin Waves*; Doniach, S., Ed.; North Holland: Amsterdam, 1968; Chapter 6.

(29) (a) Cooper, B. R. *J. Magn. Magn. Mater.* **1982**, *29*, 230. (b) Yang, D.; Cooper, B. R. In *Crystalline Electric Field Effects in f-Electron Magnetism*; Guertin, R. P., Suski, W., Żołnierek, Z., Eds.; Plenum: New York, 1982; pp 381−392.

near T_C. We must admit the fact that the residual resistivity ratio (RRR) is small and the absolute value of $\rho(T)$ is large like that for the metallic system, but it is not strange for intermetallic U-based compounds. For instance, samples of U_2Pt_2In[30,31] and $UCo_{0.5}Sb_2$[32] have been reported to show similar magnitudes of RRR and $\rho(T)$. In these compounds, Kondo effect, electron localization, and layer-type structure have been considered to play a key role among other parameters like atomic disorders and microcracks influencing also the resistivity values. These latter factors presumably result in a large value of the residual resistivity of $U_2ScB_6C_3$ ($\sim$437 $\mu\Omega$-cm). Taking into account the resistivity of the phonon reference $Th_2ScB_6C_3$, we evaluated the magnetic resistivity ($\rho_{mag} = \rho_{U2ScB6C3} - \rho_{Th2ScB6C3} - \rho_{residual}$), shown in the inset of Figure 10.

The low temperature dependence of ρ_{mag} could be fitted to the equation

$$\rho_{mag}(T) = AT^2 + bT\left(1 + \frac{2k_BT}{\Delta}\right)\exp\left(-\frac{\Delta}{k_BT}\right) \qquad (8)$$

where the first term is a Fermi-liquid-like contribution and the second term accounts for the electron-magnon scattering process.[33] Using this equation, we could obtain a satisfactory fit in the temperature range 2−15 K, with the following parameters: $A = 0.059$ $\mu\Omega$-cm/K^2, $b = 0.12(1)$ $\mu\Omega$-cm/K, and $\Delta/k_B = 70(5)$ K. From the obtained A and previously estimated γ values, we can evaluate the Kadowaki-Woods ratio $r_{KW} = A/\gamma^2$.[34] For $U_2ScB_6C_3$ r_{KW} amounts to 3.69 × 10^{-5} $\mu\Omega$-cm/(mJ/mol·K^2)^2, being almost 4 times larger than the universal value of 1 × 10^{-5} $\mu\Omega$-cm/(mJ/mol·K^2)^2 for the strongly correlated electron systems. One of the possible reasons for such a strong electron−electron scattering is the spin fluctuation present in the studied compound.

Electronic Band Structure Calculations. The results of electronic band structure calculations for $Th_2ScB_6C_3$ are presented in Figure 11. As can be seen, the occupied band states are about 0.7 Ry wide. The main peak centered at 0.6 Ry is formed by hybridized 6d Th and B 2p and C 2p bands. The 6d Th band is mainly located above the Fermi level and it hybridizes with the 3d Sc band assembling a flat DOS function around E_F. From the charge analysis given in Table 2, one sees that there is a charge transfer from Sc 3d to Th 5f band, resulting in an increase in charge at the Th site.

In Figure 12 the total DOS of $U_2ScB_6C_3$ and the partial for U, Sc, B, and C are shown. Clearly, the total DOS of $U_2ScB_6C_3$ is different from that of $Th_2ScB_6C_3$.

First of all, the difference is seen in a large spin polarization of the DOS of $U_2ScB_6C_3$. The polarization is due to splitting mainly in the 5f-electron states. Second, in contrast to a flat structure near E_F of $Th_2ScB_6C_3$, the electronic structure of $U_2ScB_6C_3$ is governed by a relatively high amplitude and a narrow band with a bandwidth of about 0.04 Ry, located just below E_F. Third, the hybridization between U-5f and U-6d with Sc-3d states in $U_2ScB_6C_3$ is smaller. Finally, concerning the hybridized bands at about 0.65 Ry and compared to 0.6 Ry in $Th_2ScB_6C_3$, one finds an upward shift in energy by about 0.05 Ry. This shift is due to the hybridization of U-6*d* with B- and C-2*p* bands. In Table 2 the calculated electrons in atomic spheres are also given for $U_2ScB_6C_3$. The fact that the uranium atom contains 2.353 *f* -like electrons may indicate a large charge transfer from U-5f to the conduction band. The observed difference in the electron numbers in atomic spheres for the Sc, B and C atoms between $Th_2ScB_6C_3$ and $U_2ScB_6C_3$ suggests a reduction of the p-d hybridization in the latter compound.

We calculated electronic specific heat coefficient γ_{theo} and then estimated the total electron-mass enhancement, $\lambda = \gamma_{exp}/\gamma_{theo} - 1$ for $Th_2ScB_6C_3$ and $U_2ScB_6C_3$ (Table 3). We see that in $Th_2ScB_6C_3$ the mass enhancement is small, whereas in $U_2ScB_6C_3$ it is significant. In fact, λ contains enhancements, which were not taken into account during the calculations, e.g., the electron−electron, electron−magnon, and electron−phonon interactions. An important result from the band structure calculations is the estimated magnetic

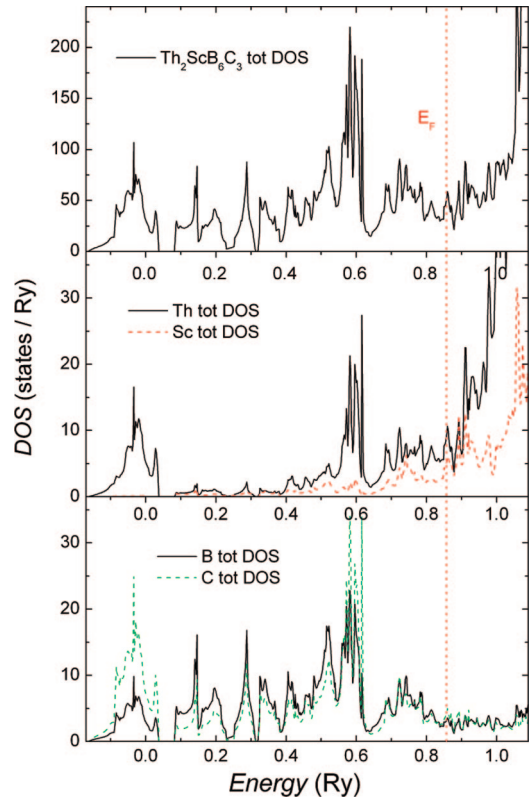

Figure 11. Total density of states (DOS) of $Th_2ScB_6C_3$ (upper panel) and partial DOS of Th/Sc (middle panel) and of B/C (bottom panel).

Table 2. Electrons in Atomic Spheres for $Th_2ScB_6C_3$ and $U_2ScB_6C_3$ in ()

atoms\orbital	s	p	d	f
Th	1.983	5.185	0.610	0.405
(U)	2.000	5.404	0.710	2.353
Sc	2.000	5.737	0.723	
(Sc)	2.000	5.749	0.774	
B	0.301	0.599		
(B)	0.306	0.628		
C	0.631	1.238		
(C)	0.638	1.256		

(30) Strydom, A. M.; du Plessis, P. de V. *Physica B* **1997**, *230−232*, 62.
(31) Estrela, P.; Naka, T.; de Visser, A.; de Boer, F. R.; Pereir, L. C. J.; Almeida, M. *Physica B* **2000**, *281−282*, 381.
(32) Tran, V. H.; Troć, R.; Bukowski, Z.; Badurski, D.; Sułkowski, C. *Phys. Rev. B* **2005**, *71*, 094428.
(33) Anderson, N. H.; Smith, H. *Phys. Rev. B* **1979**, *19*, 384.
(34) Kadowaki, K.; Woods, S. B. *Solid State Commun.* **1996**, *99*, 457.

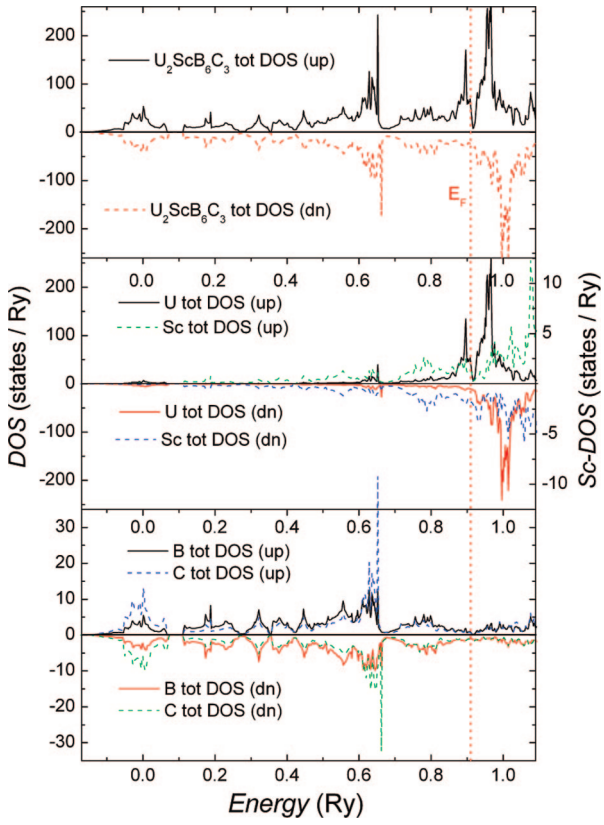

Figure 12. Total density of states (DOS) with the spin-up and spin-down functions of $U_2ScB_6C_3$ (upper panel) and partial DOS of U/Sc (middle panel) and of B/C (bottom panel).

Table 3. Calculated γ_{theo} and γ_{exp} Electronic Specific Heat Coefficients (mJ/mol.at·K^2), Electron-Mass Enhancement λ, and the Calculated Magnetic Moment M_{theo} (μ_B/U)

compounds	γ_{theo}	γ_{exp}	λ	M_{theo}
$Th_2ScB_6C_3$	3.6	4.5	0.25	
$U_2ScB_6C_3$	7.8	40	4.13	1.37

moment on uranium sites, which amounts to about M_{theo} = 1.37 μ_B/U. The main reason why the theoretical value M_{theo} is larger than the experimental one ($\sim$1 μ_B) is that we have not included in the calculations the effect of orbital contributions, which usually give the orbital moment with the direction opposed to the spin moment.

Summary

In this work we have presented X-ray single-crystal and X-ray powder diffraction data for $U_2ScB_6C_3$. Together with crystallographic data obtained on $Th_2ScB_6C_3$, we conclude that both $(U,Th)_2ScB_6C_3$ are ordered and truly quaternary compounds. The crystal structures of these compounds are typical nonmetal layer metal boron carbide compounds M_2BC. Metal atoms in $z = 0$ form a planar hexagonal net of uranium atoms centered by the smaller scandium atoms. Nonmetal atoms are found in planar Kagomé nets 6B.(6B + 3C)^2 in $z = {}^1/_2$. The nonmetal layer is centered around the metal atoms so that the hexagons of boron atoms frame the smaller scandium atoms, and the rings of 6B + 3C atoms are surrounding the larger uranium atoms. Whereas boron atoms are in tetraka-idekahedral co-ordination of $[U_4Sc_2B_2C]B$, carbon atoms are at a single-bond distance of d_{B-C} = 0.1483 nm in rectangular metal co-ordination of four uranium atoms plus two boron atoms in form of a rectangular bipyramid. The two-dimensional nonmetal network corresponds to the one in ThB_2C and forms a link to the simple structure of AlB_2 type. We believe that the reported crystallographic data of $U_2ScB_6C_3$ will be helpful in searching for new members of the quasi-two-dimensional quaternary 2163-family containing actinoid and rare-earth elements.

We have measured magnetization, specific heat, and electrical resistivity for $U_2ScB_6C_3$. The data indicate that $Th_2ScB_6C_3$ is a nonmagnetic compound and exhibits low-lying optical modes with Θ_{E1} = 173(3) K, n_{E1} = 1.6 and Θ_{E2} = 99(2) K, n_{E2} = 0.4. The uranium compound has been found to show an enhanced electronic specific heat coefficient at low temperatures ($\approx$40 mJ/mol$_U$·K^2) and to undergo successive magnetic phase transitions at T_C = 61(0.5) K and $T^* \approx$ 45 K. The origin of the latter transition is probably related to a spin reorientation of the magnetic uranium ions. The quasi-two-dimensional $U_2ScB_6C_3$ compound is characterized by an easy-plane anisotropy, which is evidenced by the experimental data and is consistent with the two-ion anisotropy interaction theory. With help of the spin-wave theory we have determined the anisotropy gap in the spin-wave spectrum $\Delta/k_B \approx 60-80$ K and the spin-wave stiffness coefficient $D \approx$ 51 meV·Å. The calculated band structures using FLAPW approach, formed for $Th_2ScB_6C_3$ and $U_2ScB_6C_3$, have indicated that the magnetism of $U_2ScB_6C_3$ is governed by the polarized 5f^3 states and a strong hybridization of the U 6d and B/C 2p states. The theoretical data confirm the metallic properties for all studied compounds and magnetic ground state in $U_2ScB_6C_3$.

Finally, the ferromagnetic ground state with an enhanced electronic specific heat coefficient implies that $U_2ScB_6C_3$ is interesting for further investigations. In contrast, the compounds USi_3 and UAl_3 with larger U−U distances of 0.40 and 0.41 nm, respectively, do not order magnetically at low temperatures, but exhibit only spin fluctuation behavior.[35,36] This comparison, with respect to the Hill limit,[24] points to an important role of the hybridization between 5f6d of uranium and p orbitals of B/C atoms in $U_2ScB_6C_3$. Further indication of the hybridization effect, providing magnetic order with some sort of spin fluctuation, is evidenced by an enhanced value of the Sommerfed ratio, i.e., 40 mJ/mol·K^2, i.e., in the same magnitude as found in spin fluctuators USi_3 (14 mJ/mol·K^2)[35] and in UAl_3 (43 mJ/mol·K^2).[36]

Acknowledgment. V.H.T. thanks the Ministry of Science and Higher Education in Poland for support with Grant No. N202 082 31/0449. V.H.T. and P.R. acknowledge the support from an Austrian Polish Scientific Exchange Program under Project 10/2006.

CM801267A

(35) Brodsky, M. B. *Rep. Prog. Phys.* **1978**, *41*, 103.
(36) Cornelius, A. L.; Arko, A. J.; Sarrao, J. L.; Thompson, J. D.; Hundley, M. F.; Booth, C. H.; Harrison, N.; Oppeneer, P. M. *Phys. Rev. B* **1999**, *59*, 14473.